

AD-A138 068

BURIED ANTENNA ANALYSIS AT VHF PART 1 THE BURIED
HORIZONTAL ELECTRIC DIPO. (U) AIR FORCE INST OF TECH
WRIGHT-PATTERSON AFB OH SCHOOL OF ENGI. J W BURKS
JAN 84 AFIT/GE0/EE/83D-1-PT-1

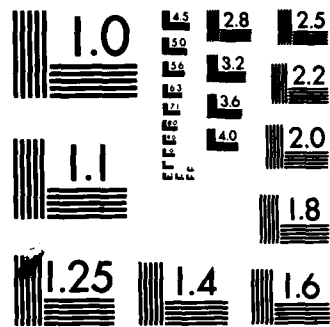
1/1

UNCLASSIFIED

F/G 9/5

NL

END
1
2
3
4
5
6
7
8
9
10
11
12



MICROCOPY RESOLUTION TEST CHART
NATIONAL BUREAU OF STANDARDS-1963-A

AFIT/GEO/EE/83D-1

BURIED ANTENNA ANALYSIS AT VHF

PART I: THE BURIED HORIZONTAL ELECTRIC DIPOLE

THESIS

AFIT/GEO/EE/83D-1

Jeffrey W. Burks
2dLt USAF

Approved for public release; distribution unlimited

DIC
DIRECTOR

FEB 22 1984

A

AFIT/GEO/EE/83D-1

BURIED ANTENNA ANALYSIS AT VHF
PART I: THE BURIED HORIZONTAL ELECTRIC DIPOLE

THESIS

Presented to the Faculty of the School of Engineering
of the Air Force Institute of Technology
Air University
In Partial Fulfillment of the
Requirements for the Degree of
Master of Science in Electrical Engineering

by

Jeffrey W. Burks, B.S.

2dLt USAF

Graduate Electro-Optics

January 1984

SEARCHED	<input checked="" type="checkbox"/>
SERIALIZED	<input type="checkbox"/>
INDEXED	<input type="checkbox"/>
FILED	<input type="checkbox"/>
FEB 1 1984	
AFIT	
Special	
A-1	

Approved for public release; distribution unlimited



Preface

The main purpose of the thesis is to aid the education process. It is a big project and many times I lost sight of the educational value and only concentrated on completing the requirements. But as I look back, I can see how much I have learned. Even though it took a little longer than I thought, the experience and knowledge gained were well worth it.

I wish to thank my advisor, Captain Thomas W. Johnson and my sponsor, Captain Torgeir G. Fadum for their help and patience. I also want to thank my church, who gave me the encouragement I needed to get this completed. Finally, I want to praise the Lord, for through Him, all things are possible (Matthew 19;26).

Jeffrey W. Burks

Contents

	<u>Page</u>
Preface.....	ii
List of Figures (Part I).....	v
List of Tables (Part I).....	v
List of Symbols.....	vi
Abstract.....	ix
 <u>Part I: The Buried Horizontal Electric Dipole</u>	
I. Introduction.....	I-1
Problem.....	-1
Definition of the Far-Field.....	-1
Development.....	-2
II. Literature Review.....	II-1
Sommerfeld Method.....	-1
Moment Method and Others.....	-5
III. Perfect Dielectric Method.....	III-1
IV. Results.....	IV-1
Vaziri.....	-1
Biggs and Swarm.....	-2
Computer Program for the Dielectric Method.....	-3
Calulated Patterns.....	-4
Directivity and Gain.....	-9
Losses.....	-10
V. Conclusions and Recommendations.....	V-1
Conclusions.....	-1
Recomendations.....	-1
Bibliography.....	BIB-1
Appendix A: Vaziri's Program.....	A-1
Appendix B: Dielectric Method Program	B-1
Vita.....	VIT-1

Contents

	<u>Page</u>
List of Figures (U)	xi
 <u>Part II: The Buried Array - Analysis of the SCOT Antenna</u>	
VI. Introduction to the SCOT Antenna (U)	VI-1
Design and Characteristics of the SCOT Antenna (U)	-1
Scope and Assumptions (U)	-6
Development (U)	-8
VII. Review of Corvus (U)	VII-1
Elemental Dipole Factor (U)	-1
Segment Factor (U)	-3
Element and Array Factors (U)	-7
Coupling Between Segments (U)	-7
VIII. British Study (U)	VIII-1
IX. Results (U)	IX-1
Measurements (U)	-1
Calculated Pattern (U)	-1
X. Conclusions and Recommendations (U)	X-1
Conclusions (U)	-1
Recommendations (U)	-1
Bibliography (U)	BIB-5

List of Figures

<u>Figure</u>	<u>Page</u>
III-1. Orientation of the HED in an Infinite Dielectric Medium.....	III-3
III-5. Orientation of the HED Showing the Air-dielectric Interface and Ray Paths.....	III-5
IV-1. Calculated Pattern for the HED, Both in Free Space and Buried.....	IV-5
IV-2. Calculated Pattern for the Buried HED With Different Soil Dielectric Constants.....	IV-6
IV-3. Calculated Pattern for the Buried HED With Different Antenna Attenuation Coefficients ($\epsilon_g = 9.0$).....	IV-7
IV-4. Calculated Pattern for the Buried HED With Different Antenna Propagation Constants ($\epsilon_g = 9.0$).....	IV-8

List of Tables

<u>Table</u>	<u>Page</u>
III-1. The Complex Index of Refraction at 37.5 MHz for Different Soils.....	III-2
IV-1. Soil Losses at a Burial Depth of 0.5 Meters.....	IV-11

List of Symbols

AF	array factor
$d\Omega$	differential solid angle (steradians)
D	directivity
D_m	dipole moment
E	electric field
f	frequency
G	gain
HED	horizontal electric dipole
HF	3 - 30 MHz
I	current
I_{dl}	dipole moment for infinitesimal antenna
j	$\sqrt{-1}$
k	propagation constant
L	length of antenna
LF	30 - 300 kHz
n	index of refraction
P	power
R	distance from antenna (meters)
t	transmission coefficient for the electric field
T	transmission coefficient for power
U	radiation intensity (Watts/steradian)
VHF	30 - 300 MHz
VLF	3 - 30 kHz

α	antenna attenuation coefficient (nepers/meter)
γ	phase factor
γ_1	loss factor
ϵ	permittivity
η	intrinsic impedance
θ	angle off the normal to the interface
λ	wavelength (meters)
μ	permeability
ξ	angle off horizon
π	3.1415926536
ρ	reflection coefficient for the electric field
σ	conductivity (mhos/meter)
ϕ	azimuthal angle
ϕ	phase of current at $x = 0$
ψ_1	$jk_0 \cos \xi \cos \phi$
ω	radial frequency (radians/second)

Subscripts

a	air
ave	average
bs	Biggs and Swarm method
g	ground
in	input
o	free-space
r	relative to free-space
s	segment factor

t transmitted
θ θ-polarization
φ φ-polarization
L on antenna

Example: E_g - electric field in the ground

Abstract

Part I:

A method was developed to find the far-field radiation pattern of a buried horizontal electric dipole (HED) at 37.5 MHz. The imaginary part of the index of refraction was shown to be negligible for dry soil at this frequency so standard antenna theory and ray-optic theory were used. The effect of the ground-air interface was modeled using the transmission coefficient and Snell's law for a dielectric interface. Because the current distribution for the buried HED depends on antenna construction, results are shown for the far-field pattern in the air for different current distributions on the HED.

The literature on this problem was reviewed; most used the Sommerfeld or moment methods to make the same calculations. The results of one of the reports using the Sommerfeld method could be compared and were found to be similar. An extensive bibliography is included.

Part II:

The analysis was then applied to a buried antenna array. The current distribution was known and was used to calculate the far-field pattern. It was concluded that the far-field pattern is highly dependent on the current distribution. This part is classified.

I. Introduction

The theory of antennas, both in free space and above a conducting ground plane has been well defined and tested. When an antenna is buried in a medium such as the ground, the nature of the antenna is changed. The radiation pattern, current distribution, impedance and other parameters can no longer be calculated by the usual methods.

Problem

To analyze the effectiveness of a buried antenna array, the far-field pattern must be determined. The goal of this thesis is to develop a simple but accurate method to determine this pattern. The antenna array to be studied is made up of horizontal electric dipoles (HED's) and operates at 37.5 MHz. The HED's are a half-wavelength long (4 meters). The exact arrangement of the array is classified and is discussed in Part II.

Definition of the Far-Field

The far-field condition is $R \gg D$ where R is the observation distance and D is the largest dimension of the antenna. The far-field considered in this study does not include the fields in the ground. Those fields are attenuated at a rate greater than $1/R$. The attenuation is dominated by the lossy effects of the ground over which it travels. The ground wave thus is insignificant for long ranges

from the antenna. Therefore in this study it is necessary to compute only the space wave for the far-field pattern. Its fields vary as a function of $1/R$ and travel away from the surface.

Development

A review of the applicable open literature is given in Chapter II. In this study, the radiation equation for an antenna in free space is applied to this problem using ray-optics and Snell's law at the ground-air interface. This is presented in Chapter III. Chapter IV shows the results of computations of the pattern for different parameters using the methods from Chapters II and III. Finally, Chapter V gives conclusions and recommendations for further study.

II. Literature Review

There are many studies of buried antennas in the open literature. Many of them analyze the buried HED at lower frequencies. It was difficult to apply the results to this application because the assumptions and approximations are implicit in the mathematical derivations. This is primarily due to the complexity of modeling the conductive half-space of the ground. Most of the studies reviewed here are based on Sommerfeld's method.

Sommerfeld Method

A. Sommerfeld did the initial work in this area in the early 1900's (Ref 1) and his method is followed today. A quick summary is given here before moving on to the specific articles.

The Sommerfeld method obtains an exact integral representation of the fields in adjacent conductive half-space and lossless half-space. The Helmholtz equation

$$(\nabla^2 + k^2)\bar{\Pi} = -jI\delta l\eta/k \quad (2-1)$$

is solved by a Fourier-Bessel transform using the appropriate boundary conditions. The fields are obtained using

$$\bar{E} = \nabla(\nabla \cdot \bar{\Pi}) + k^2\bar{\Pi} \quad (2-2)$$

$$\bar{H} = \frac{-jk}{\eta} \times \bar{\Pi} \quad (2-3)$$

It is fairly simple to show that equations (2-1), (2-2), and (2-3) are a solution to Maxwell's equations. The inverse Fourier-Bessel transform can then be found by an asymptotic approximation, which results from a

suitable integration in the complex plane.

Several reports have been written by Biggs and Swarm that use the Sommerfeld method (Ref 2-5). They calculate both the near and far fields from a buried HED operating at VLF (3-30 kHz) or LF (30-300 kHz). They state that propagation is limited to low frequencies because of losses, but it is not expressed as a formal limitation of the results.

Biggs (Ref 2) analyzes an inclined dipole in a conducting medium. He assumes that the depth of burial is much less than the observation distance. He also assumes that $n_g^2 \gg 1$ and $k_a R/n_g^2 > 1$, where n_g is the complex index of refraction of the ground, k_a is the propagation constant of the air, and R is the observation distance.

Biggs and Swarm (Ref 3) analyze the HED in a conducting medium. The real part of the complex index of refraction is neglected, assuming

$$\frac{\sigma_g}{\omega \epsilon_0} \gg \epsilon_r \quad (2-4)$$

This a poor approximation at VHF (30-300 MHz) as will be shown in Chapter III. Biggs and Swarm (Ref 4) give results for the HED in a lossy dielectric consisting of ice or soil. The condition in this report is that

$$R \sin \theta_a \gg \frac{n_g^2}{k_a} \quad (2-5)$$

where θ_a is the angle in the air off the normal to the ground. This article is a summary of an earlier report (Ref 5) that goes into more detail on the mathematical analysis. In these last three reports (Ref 3-5), there is no limitation given for the depth of burial.

The electric fields are given as functions of polarization, distance, and position for all 4 reports (Ref 2-5) for both space waves

and ground waves. The equations are similar and are compared in Chapter IV.

Entzminger et al (Ref 6) use the same space wave equations as given in Biggs and Swarm (Ref 4.205) to calculate fields for a buried HED operating over the entire HF (3-30 MHz) range. They also study the gain and impedance of an insulated wire antenna. Several antennas of this type were constructed and buried 1 to 3 feet deep in an open field. Both the space wave and the ground wave patterns were measured for frequencies of 2 to 10 MHz. They cite excellent agreement between theoretical and measured values.

The Sommerfeld method is explained in detail by Baños (Ref 7). He calculates both the near and far fields for a HED at any depth of burial. He assumes LF operation in a conducting medium such that the real part of the complex index of refraction is negligible. (A special note - 'n' in his book represents the reciprocal of the index of refraction for the ground.)

Vaziri (Ref 8) uses the Sommerfeld method to analyze all four Hertzian dipoles, horizontal and vertical electric dipoles and horizontal and vertical magnetic dipoles, as buried antennas. Rather than obtaining the inverse Fourier-Bessel transform asymptotically, he evaluates the inversion integral by direct numerical integration in the complex plane. His Fortran program is given but its limitations are not discussed. Its purpose is to calculate the E and H-fields at any polarization at any observation point in a certain plane. For the HED, this plane is the vertical plane parallel to and intersecting the dipole. Above ground antennas can also be modeled by switching the medium constants around.

Experimental results are given for a horizontal traveling wave antenna buried 40 centimeters deep in an open field and operated at 144 MHz. The theory and measurements agreed within the "acceptable accuracy". Also, Baños's approximations are computed in the program and are also found to agree with the measurements in most cases. This is surprising because they are not supposed to be valid for such high frequencies.

King, Sandler, and Shen (Ref 9) use the Sommerfeld method to find the fields in the ground for a buried HED. The fields in the air are not examined. Both a complex permittivity and complex conductivity are used to calculate the propagation constant of the ground, k_g .

King and Shen (Ref 10) use the Sommerfeld method to calculate the fields directly above a buried HED to determine its environmental hazard. Graphs are given for the fields at a height z from a HED buried 0.175 meters in dry soil and operated at 144 MHz. But the values given for conductivity ($\sigma_g = 4 \times 10^{-5}$ mhos/meter) and permittivity ($\epsilon_g = 4\epsilon_0$) do not satisfy the condition that

$$\frac{k_a}{k_g} \leq 0.05 \text{ (ie } n_g \geq 20) \quad (2-6)$$

where

$$k_a = \omega(\mu_0\epsilon_0)^{\frac{1}{2}} \quad (2-7)$$

$$k_g = (\omega^2\mu_0\epsilon_g + j\omega\mu_0\sigma_g)^{\frac{1}{2}} \quad (2-8)$$

For these values of σ_g and ϵ_g , the imaginary part of k_g is at least an order of magnitude smaller than the real part for frequencies above 2 MHz. So at 144 MHz,

$$k_g \approx (4\mu_0\epsilon_0)^{\frac{1}{2}} \quad (2-9)$$

Therefore,

$$\frac{k_a}{k_g} = 0.5 \quad (2-10)$$

which is a factor of 10 too big.

A different approach is given by Bannister (Ref 11) that combines the Sommerfeld method with image theory. He gives equations for the far-field and requires that $n_g^2 > 15$. He also requires that the observation distance be at least three times greater than the burial depth. A few results are given for the HF range, but there seems to be no other restrictions on frequency.

In all the reports mentioned so far (Ref 2-11), the current distribution on an actual antenna is not analyzed. Calculations are performed only for an infinitesimal dipole, with a uniform current distribution. Entzminger et al (Ref 6.7) do replace the dipole moment, $I dl$, by a general dipole moment,

$$D_m = \int_{-L/2}^{L/2} I(x) \exp(jk_0 x \cos \phi) dx \quad (2-11)$$

but does not evaluate it. Also, this dipole moment is only valid for the fields at the surface.

Moment Method and Others

The moment method has been applied to the buried antenna problem to find the pattern without knowing the current distribution. Miller and Burke (Ref 12) and Miller and Deadrick (Ref 13) use the moment method on the thin wire integral equations along with a transmission coefficient for a buried HED. They report their results to be consis-

tent with the Sommerfeld method. It seems to be applicable to VHF but the mathematics are outside the scope of this thesis. Numerical results are given in Reference 13 for a buried wire antenna operated at frequencies of 1 MHz and 10 MHz.

Brammer (Ref 14) presents the moment method and a transmission line method as two ways to calculate the fields for a buried insulated wire antenna operated at 2 to 16 MHz. The methods and assumptions are not described very well but he reports them to be consistent.

Many other references to buried antennas were found but only the ones that are discussed here apply directly to the problem of finding the far-field pattern of a buried HED. Some of these other references are listed (Ref 18-43) for future reference.

III. Perfect Dielectric Method

If the ground is assumed to be a perfect or slightly lossy dielectric ($\epsilon'' \ll \epsilon'$), standard ray-optics and antenna theory can be used to calculate the far-field antenna pattern for a buried antenna. Table III-1 shows the complex index of refraction,

$$\tilde{n}_g = \sqrt{\epsilon_r - j \frac{\sigma}{\omega \epsilon_0}} \quad (3-1)$$

for different soils with $\omega = 2\pi \times 37.5$ MHz. For dry conditions, the imaginary part of \tilde{n}_g can be neglected and the slightly lossy dielectric assumption holds. For these values and at this frequency, the assumption is not very good for wet soils.

Assuming dry soil, the field distribution of the buried antenna can now be calculated by standard techniques. The method in Stutzman and Thiele (Ref 15.25) is modified to account for the air-dielectric interface. The E-field at some far-field point Q for a dipole of length L on the x-axis as shown in figure III-1 is

$$\vec{E}_g = - \frac{j\omega\mu_g}{4\pi R} (\cos\theta_g \cos\phi \hat{\theta} - \sin\phi \hat{\phi}) D_m \exp(-jk_g R) \quad (3-2)$$

where

$$D_m = \int_0^L I(x) \exp(jk_g x \sin\theta_g \cos\phi) dx \quad (3-3)$$

$$k_g = n_g k_0 \quad (3-4)$$

When the half-space above $z=h$ is replaced by air, the radiation observed at point Q is different due to the following:

Reference	Soil moisture content	Analysis frequency	Dielectric constant ϵ_r	Conductivity σ (mhos/m)	Complex index of refraction n_c (at 37.5 MHz)
Biggs and Swarm (Ref 3:206)	not given	LF	10	0.0005	$10 - j0.24$
Entzminger <u>et al</u> (Ref 6:45-48)	wet?	10 MHz	60	0.03	$60 - j14.0$
King and Shen (Ref 10:1052)	dry	144 MHz	4	0.00004	$4 - j0.019$
Corvus (Ref 46:33)	dry	HF, VHF	9	0.001	$9 - j0.48$
	wet	HF, VHF	25	0.01	$25 - j4.8$
Burke <u>et al</u> (Ref 47:99)	dry	HF, VHF	9	0.005	$9 - j2.4$
	wet	HF, VHF	20	0.05	$20 - j24$

Table III-1. The Complex Index of Refraction at 37.5 MHz for Different Soils.

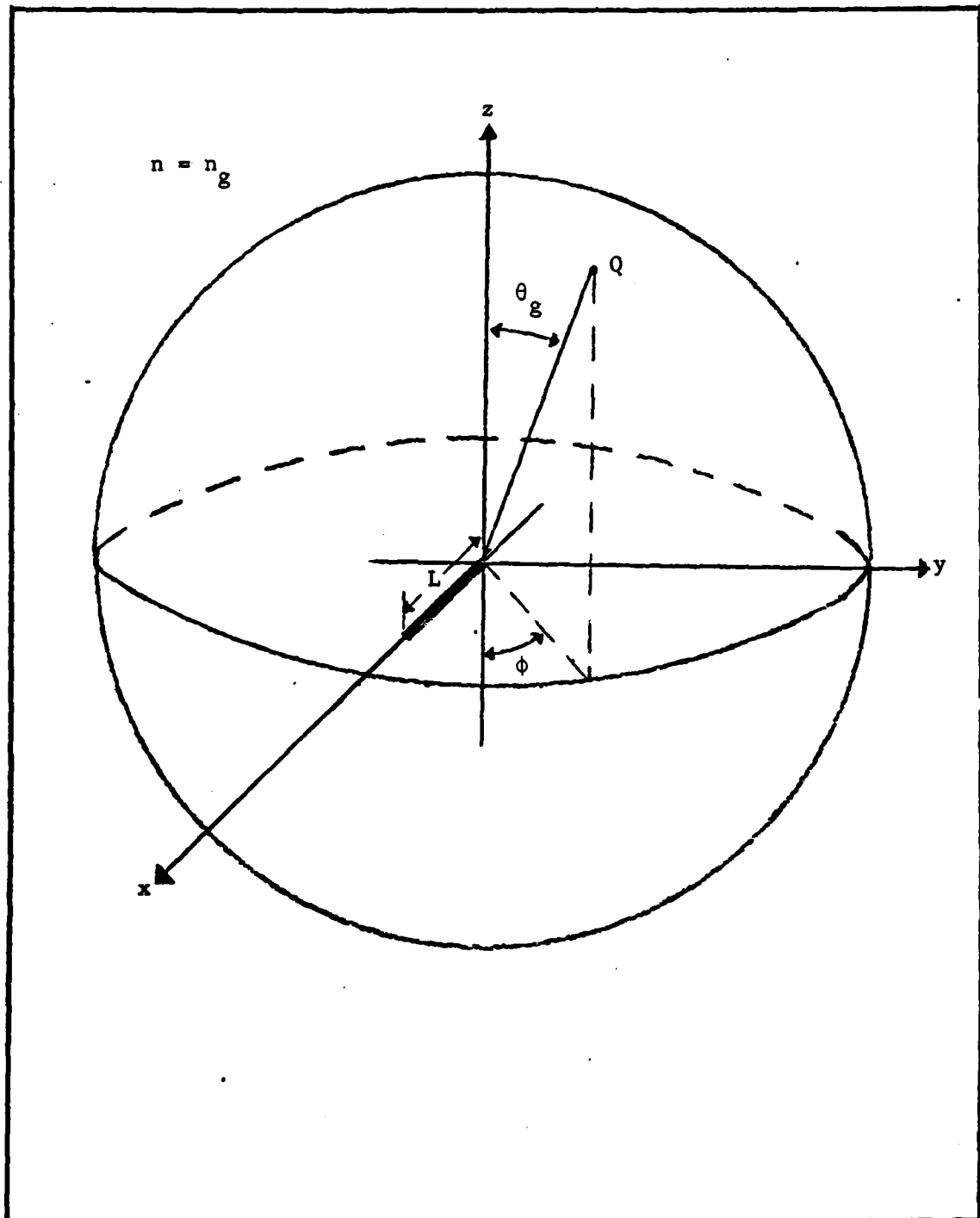


Figure III-1. Orientation of the HED in an Infinite Dielectric Medium.

- 1) Only part of the radiation incident on the interface is transmitted; the rest is reflected.
- 2) Refraction changes
 - a) the direction of the radiation,
 - b) the dipole moment, D_m , and
 - c) the radiation intensity, U_g .

The Fresnel transmission coefficient (Ref 16.74), t , is used to calculate the part of the field that is transmitted such that

$$E_{\theta t} = t_{\theta} E_{\theta g} \quad (3-5)$$

$$E_{\phi t} = t_{\phi} E_{\phi g} \quad (3-6)$$

For the θ -polarized E-field,

$$t_{\theta} = \frac{2n_g \cos\theta_g}{n_a \cos\theta_a + n_g \cos\theta_g} \quad (3-7)$$

and for the ϕ -polarized E-field,

$$t_{\phi} = \frac{2n_g \cos\theta_g}{n_a \cos\theta_a + n_g \cos\theta_g} \quad (3-8)$$

The effect of refraction is described by Snell's law

$$n_a \sin\theta_a = n_g \sin\theta_g \quad (3-9)$$

Using equations (3-4) and (3-9) in (3-3) results in

$$D_m = \int_0^L I(x) \exp(jk_0 x \sin\theta_a \cos\phi) dx \quad (3-10)$$

which is the same dipole moment as for an HED in free space. The ground has no effect because all rays at a certain angle travel the same distance through the ground as shown in figure III-2. Because array theory is derived from the free space dipole moment, this also means that conventional array theory can be used in analyzing buried

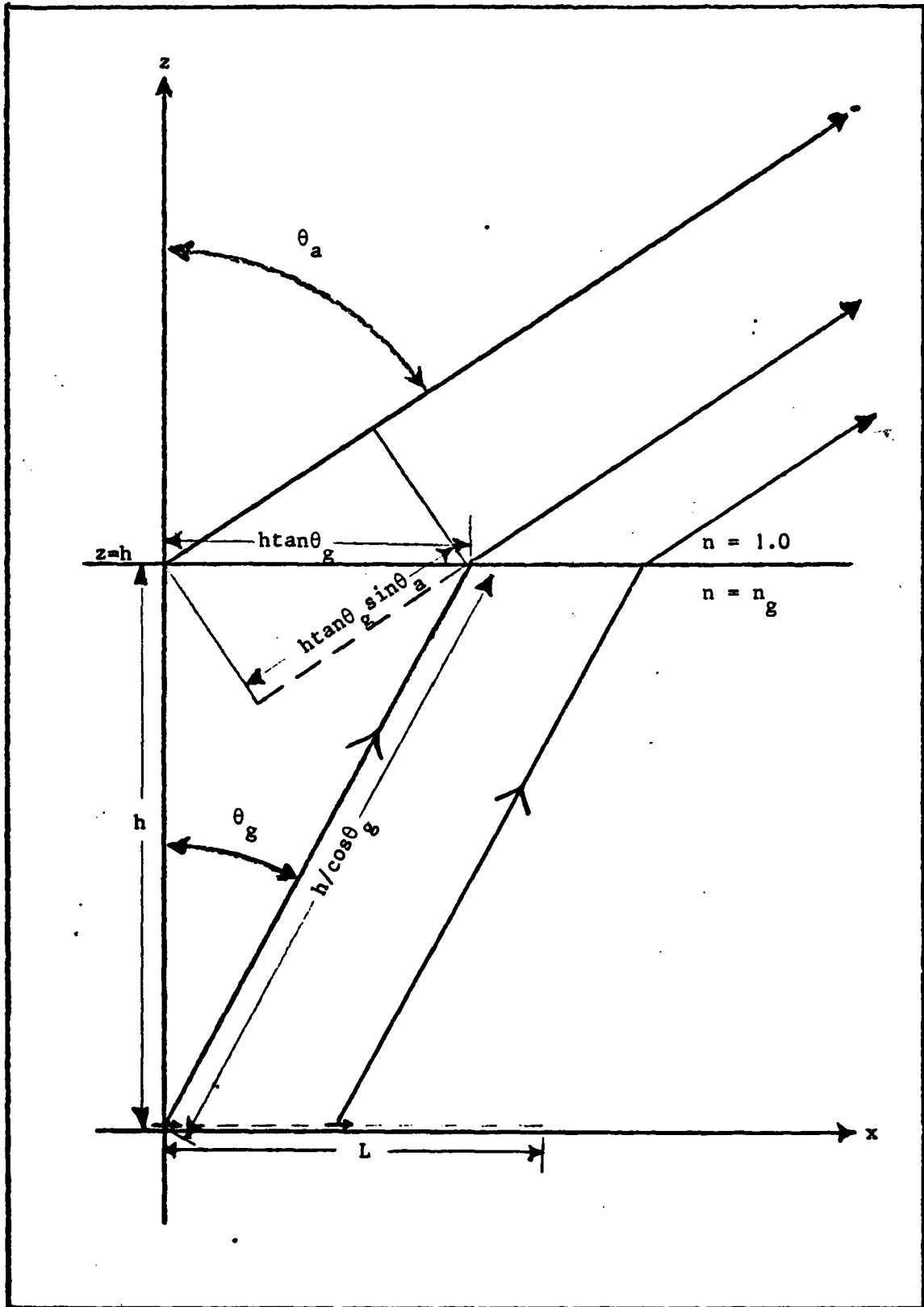


Figure III-2. Orientation of the HED Showing the Air-dielectric Interface and Ray Paths.

antenna arrays.

The phase factor, $\exp(-jk_o R)$ in equation (3-2) changes slightly to

$$\gamma = \exp\left(-\frac{jk_o n_g h}{\cos\theta_g} - jk_o (R - h \tan\theta_g \sin\theta_a)\right) \quad (3-11)$$

The wave travels a distance $h/\cos\theta_g$ through the ground, but the distance it travels through the air is shortened by $h \tan\theta_g \sin\theta_a$ as shown in Figure III-2. Equation (3-11) is then simplified to

$$\gamma = \exp(-jk_o R - jk_o n_g h \cos\theta_g) \quad (3-12)$$

by using Snell's law, a trigonometric identity, and equation (3-4).

If the losses and near-fields are ignored, then the power just above the surface in the solid angle $d\Omega_g$ must be equivalent to the power in the far-field in the solid angle $d\Omega_a$, such that

$$U_a(\theta_a, \phi) d\Omega_a = U_t(\theta_g, \phi) d\Omega_g \quad (3-13)$$

where

$$d\Omega_a = \sin\theta_a d\theta_a d\phi \quad (3-14)$$

$$d\Omega_g = \sin\theta_g d\theta_g d\phi \quad (3-15)$$

Differentiating Snell's law yields

$$d\theta_g = \frac{n_a \cos\theta_a}{n_g \cos\theta_g} d\theta_a \quad (3-16)$$

and substituting this and Snell's law into equation (3-15) results in

$$d\Omega_g = \frac{n_a}{n_g} \sin\theta_a \frac{n_a \cos\theta_a}{n_g \cos\theta_g} d\theta_a d\phi = \frac{n_a^2 \cos\theta_a}{n_g^2 \cos\theta_g} d\Omega_a \quad (3-17)$$

From equations (3-13) and (3-17)

$$U_a(\theta_a, \phi) = U_t(\theta_g, \phi) \frac{n_a^2 \cos\theta_a}{n_g^2 \cos\theta_g} \quad (3-18)$$

From Poynting's theorem, the radiation intensity is

$$\bar{U} = \text{Re}(\frac{1}{2} \bar{E} \times \bar{H}^*) R^2 \hat{R} \quad (3-19)$$

In free space or air, \bar{E} and \bar{H} are perpendicular and $H = E/\eta_0$, therefore,

$$U_t(\theta_g, \phi) = \frac{1}{2\eta_0} |E_t|^2 R^2 \quad (3-20)$$

Thus, the far-field pattern is

$$U_a(\theta_a, \phi) = \frac{t^2}{2\eta_0} |E_g|^2 \frac{n_a^2 \cos\theta_a}{n_g^2 \cos\theta_g} R^2 \quad (3-21)$$

So from equations (3-2), (3-5), (3-7), and (3-10), the far-field pattern for the θ -polarized E-field is

$$U_a(\theta_a, \phi) = \left(\frac{2n_g \cos\theta_g}{n_g \cos\theta_a + n_a \cos\theta_g} \right)^2 \left(\frac{1}{2\eta_0} \right) \left(\frac{-j\omega\mu_g}{4\pi} \cos\theta_g \cos\phi \right)^2 \frac{n_a^2 \cos\theta_a}{n_g^2 \cos\theta_g} \times \left(\int_0^L I(x) \exp(jk_0 \sin\theta_a \cos\phi) dx \right)^2 \quad (3-22)$$

where $\mu_g = \mu_0$.

Results using this equation will be shown in the next chapter after a brief look at the results from the Sommerfeld method.

IV. Results

As seen from the preceding two chapters, there are several ways of analyzing the buried antenna. The next step is to apply these methods for this specific case and compare the results. It would be even better to compare them to actual measurements, but these are unavailable at this time.

Of the three main methods; the moment method (Ref 12,13), the Sommerfeld method (Ref 2-11), and the dielectric method, only the Sommerfeld method and dielectric methods are discussed here. The moment method looks promising but is better left for another study.

Biggs and Swarm (Ref 4) and Vaziri (Ref 8) use the Sommerfeld method to give solutions that seem the most applicable here. Many of the other solutions were not usable because of the specific assumptions or conditions. Usually, the analyses applied only for lower frequencies, and hence, the index of refraction is assumed to be greater than what it is at VHF.

Vaziri

The Fortran program written by Vaziri looked very promising as mentioned before. It was typed into AFIT's Vax 11/780 computer line by line as given in his dissertation. Some of it was excluded because the code given for the vertical electric dipole and magnetic dipoles was not needed. At first, the program would not compile. No syntax or error message was generated during assembly. Only when the multiple

RETURN's were taken out of the FNC function did the program compile without generating a compiler error. Evidently, there were more RETURN's in the FNC function than the Vax could handle. When these were reduced by deleting more unneeded code, the program compiled. This version is shown in Appendix A for future reference.

When it was run with $n_g = 3.0$, $\sigma_g = 0.005$ mhos/meter, and the burial depth, $h = 0.5$ meters, the output was obviously wrong. For a distance of 50 meters, the antenna pattern increases toward infinity at an angle of 35° off the horizon. For greater distances, the angle where the pattern goes to infinity is decreased. The code was examined several times but the error was not found.

Biggs and Swarm

Biggs and Swarm give the closed form solution of the far-field θ -polarized E-field as

$$E_{bs} = \frac{j}{R} 60k_o Idl \cos\phi \frac{\cos\theta_a \sqrt{n_g^2 - \sin^2\theta_a}}{\tilde{n}_g \cos\theta_a + \sqrt{n_g^2 - \sin^2\theta_a}} \cdot \exp(jk_o R + jk_o h \sqrt{n_g^2 - \sin^2\theta_a}) \quad (4-1)$$

They have assumed that $k_o R/n_g^2 \gg 1$. This is met when $R > 100$ meters for $n_g = 3.0$. Using the same argument as for the dielectric method, the imaginary part of \tilde{n}_g can be neglected at this frequency. The radiation intensity can be calculated from

$$U_{bs} = \frac{1}{2\eta} |E_{bs}|^2 R^2 \quad (4-2)$$

(see equation (3-20)). Then from Snell's law and a trigonometric identity

$$n_g \cos\theta_g = \sqrt{n_g^2 - \sin^2\theta_g} \quad (4-3)$$

it can easily be shown that

$$U_{bs} = U_a \frac{\cos\theta_a}{\cos\theta_g} \quad (4-4)$$

where U_a is the result from the dielectric method, equation (3-22), with dipole moment Idl .

This seems to indicate that these two methods of calculating the E-fields are compatible. The results are in complete agreement at $\theta_a = 0^\circ$ (directly overhead), but diverge as the angle increases toward the horizon. For $n_g \geq 3$, $\cos\theta_g \approx 1$ for all θ_a , so the difference is mainly a factor of $\cos\theta_a$. The equations given in the other reports by Biggs and Swarm (Ref 2,3,5) as well as King and Shen (Ref 10) also give the same answer for $\theta_a = 0^\circ$.

Computer Program for the Dielectric Method

The Fortran program shown in Appendix B was developed from the equations of Chapter III and used to calculate the radiation pattern for a buried half-wave HED. Although the program will calculate both θ and ϕ -polarizations, only results for the θ -polarization are shown here for simplicity. No new information would be gained by looking at the ϕ -polarization but it might be important in a later study so the equations were left intact.

The integration to calculate the dipole moment (equation (3-10)) is performed numerically because the effect of burial on the current distribution is not known. In this way, different current distributions can be tested to see what pattern is generated.

The Uff subroutine (page B-3) can be used to calculate the far-field radiation intensity in any direction in the air above a buried

HED. Both U_a and U_{bs} are calculated given the index of refraction, θ_a , ϕ , and the parameters for the current distribution. The program should be applicable to other frequencies by changing the value of FQ (frequency) as long as the imaginary part of the index of refraction is negligible at that frequency.

Calculated Patterns

The results shown here are for the radiation intensity in the x-z plane. A sinusoidal current distribution

$$I(x) = \sin(k_r k_o x) \exp(-\alpha x) \quad (4-5)$$

was used to model the current on a 4-meter-long wire antenna.

Figure IV-1 shows the pattern for the half-wave HED, both in free-space and buried. The buried antenna radiates a much more constant pattern. Figure IV-2 shows the change in the pattern for the range of soil dielectric constants. The radiation intensity near the horizon does not change very much, but these do not take into account how the current distribution might change. Here, the current distribution was held constant, but in the real world the current distribution may change drastically.

Figures IV-3 and IV-4 show what happens as the current distribution is changed. In Figure IV-3, the current has been attenuated by changing the value of α in equation (4-5). This does not change the pattern except to lower it as the attenuation is increased. As the propagation constant is changed, the pattern changes much more, although it is still the same near the horizon as shown in Figure IV-4.

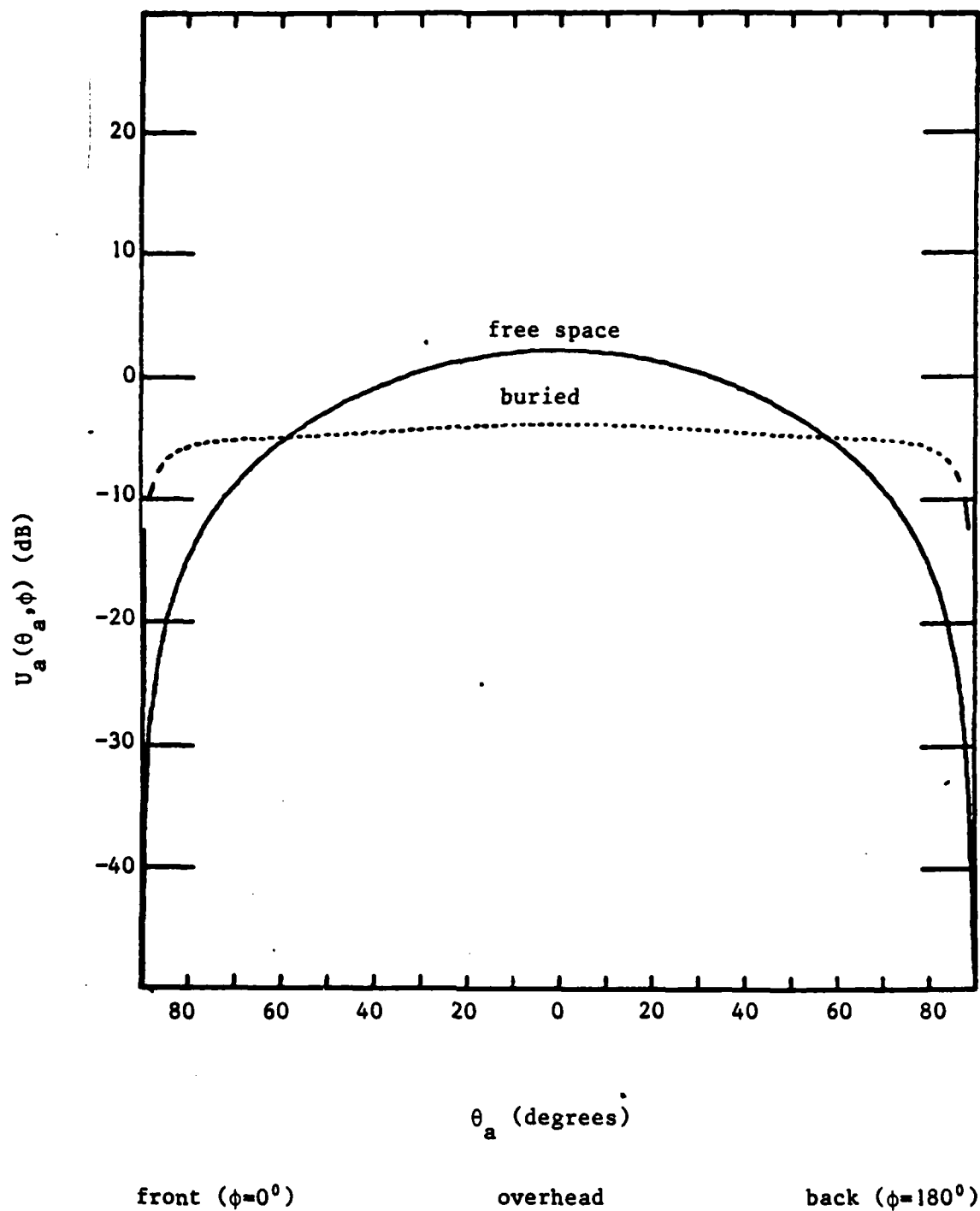


Figure IV-1. Calculated Pattern for the HED, Both In Free Space and Buried.

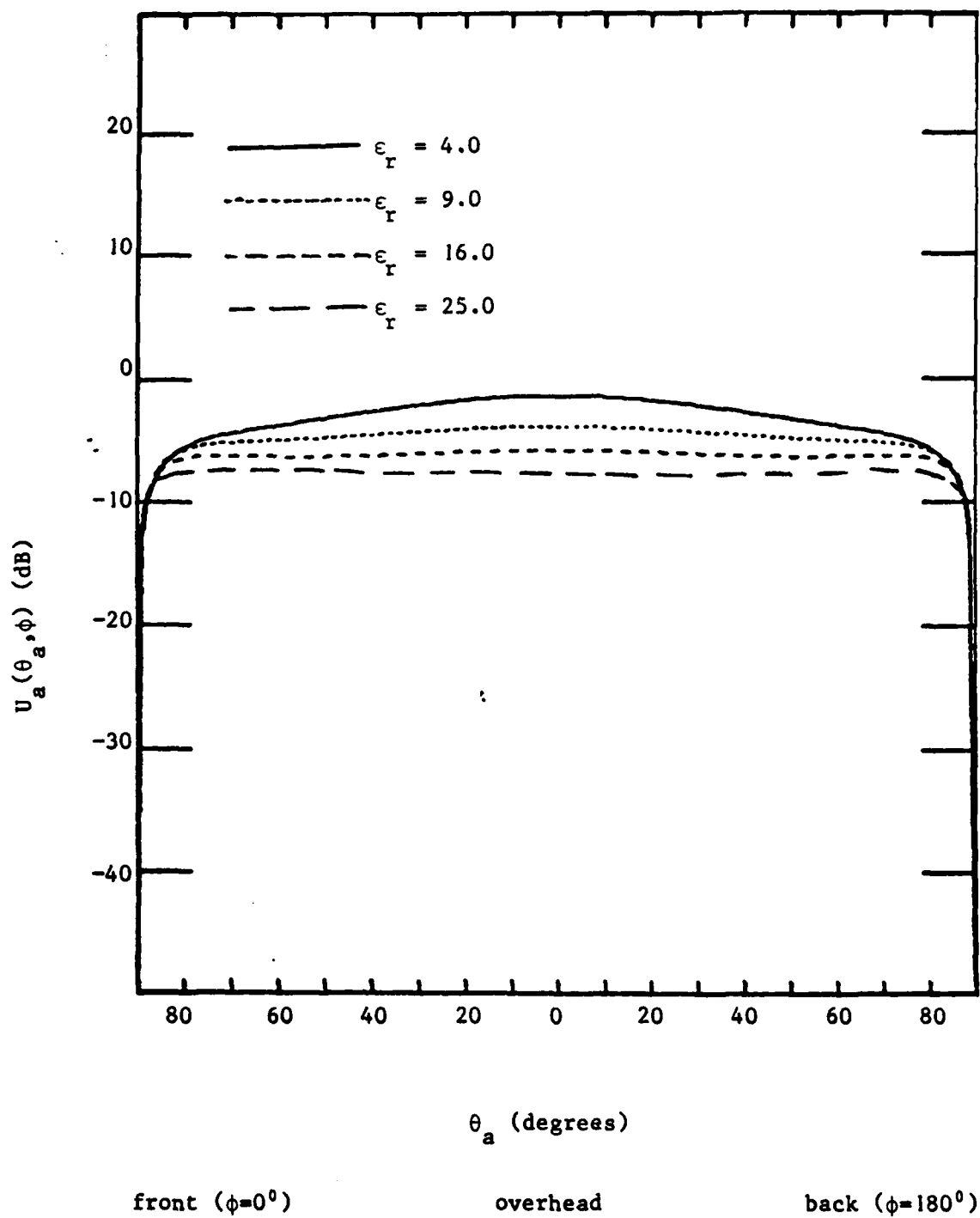


Figure IV-2. Calculated Pattern for the Buried HED With Different Soil Dielectric Constants.

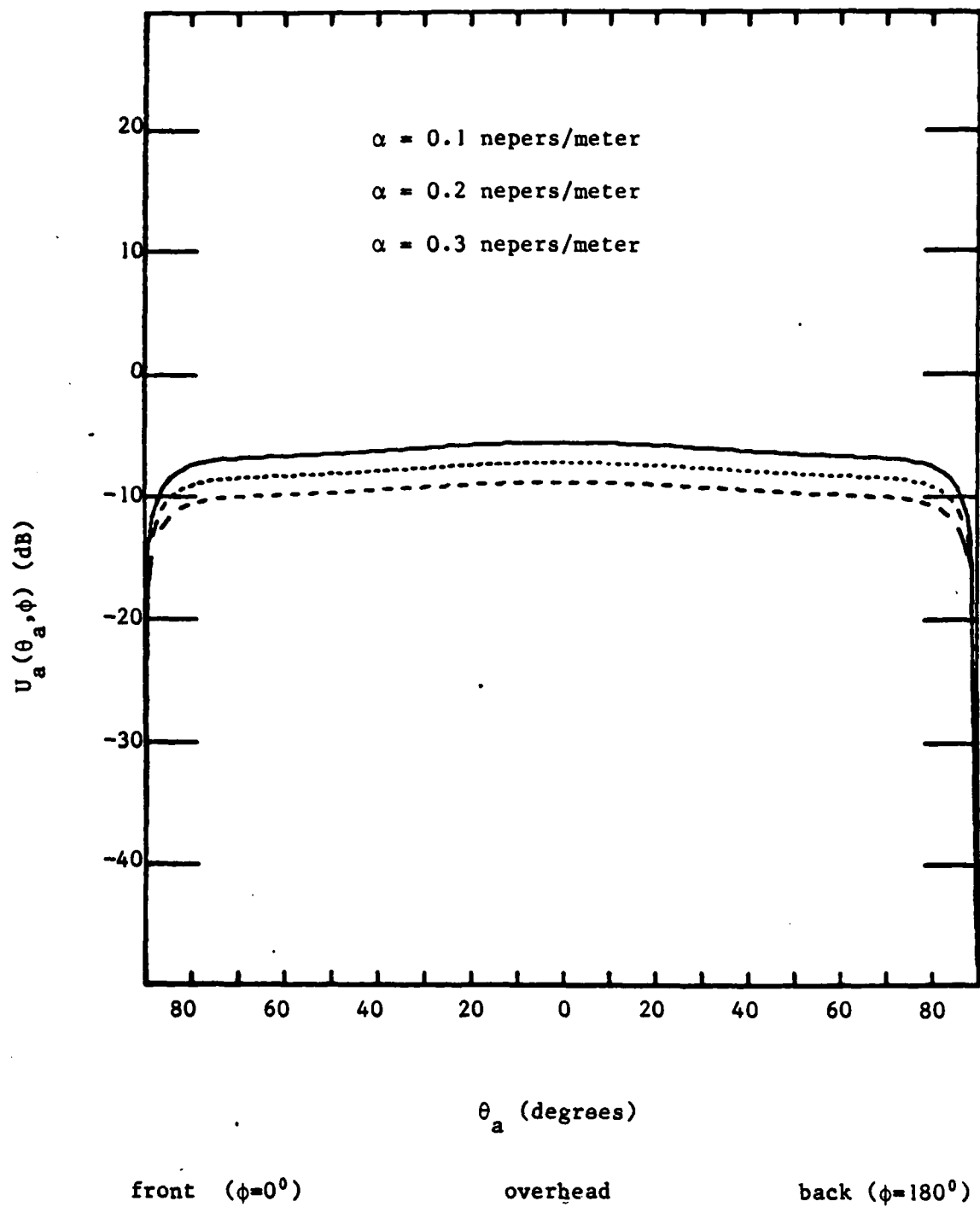


Figure IV-3. Calculated Pattern for the Buried HED With Different Antenna Attenuation Coefficients ($\epsilon_r = 9.0$)

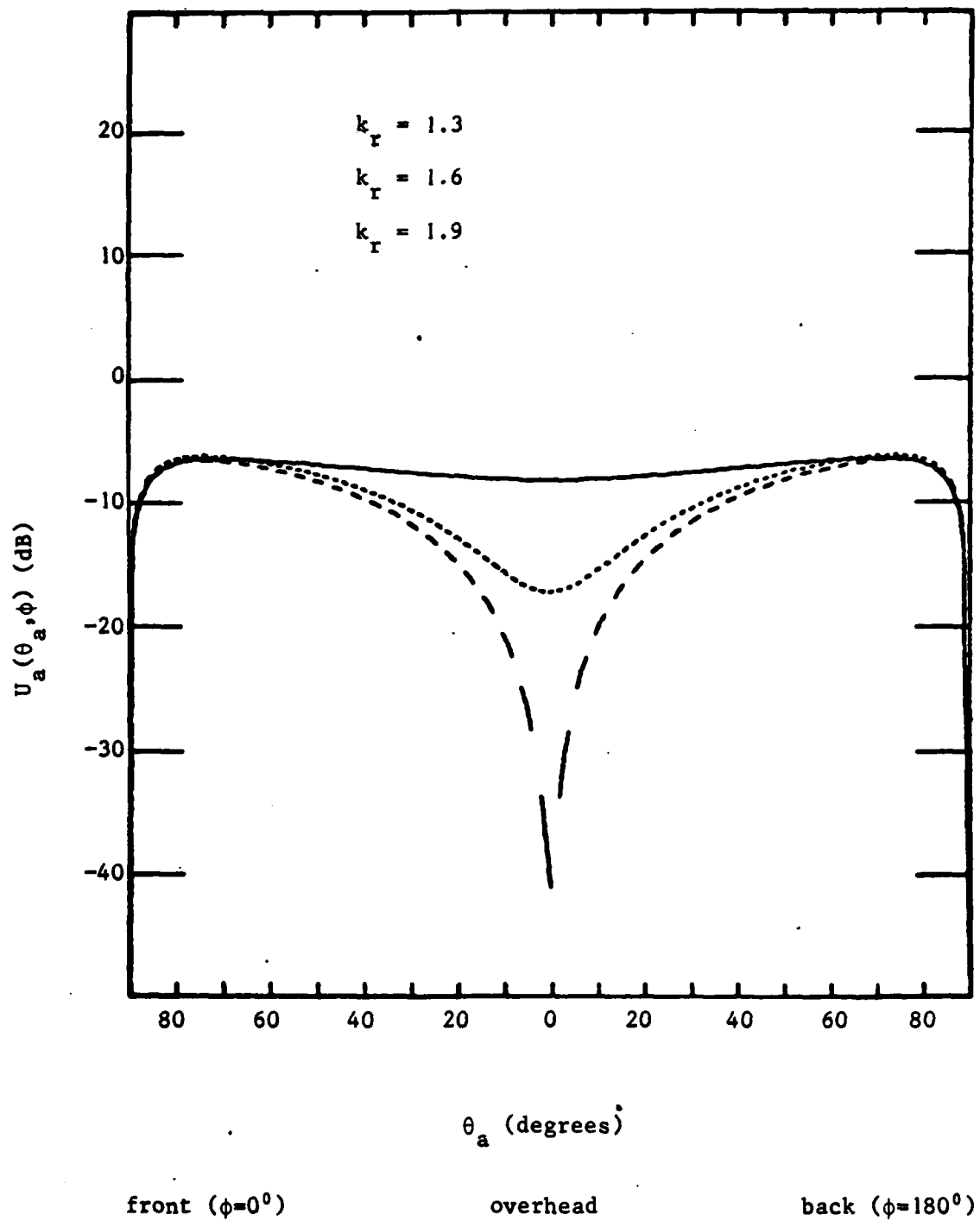


Figure IV-4. Calculated Pattern for the Buried HED With Different Antenna Propagation Constants ($\epsilon_r = 9.0$).

Directivity and Gain

It is more desirable to plot the directivity or gain rather than just the pattern. That would mean that the whole pattern would be shifted up or down according to the total amount of power radiated or used. The directivity is given by

$$D(\theta, \phi) = \frac{U(\theta, \phi)}{U_{ave}} \quad (4-6)$$

where

$$U_{ave} = \frac{1}{4\pi} P_{radiated} = \frac{1}{4\pi} \int U(\theta, \phi) d\Omega \quad (4-7)$$

To find the total radiated power, the whole pattern must be known. That includes the radiation intensity in the ground that results not only from direct radiation from the antenna, but also reflections from the interface. Then the whole pattern would have to be integrated numerically. An analytic integration would be even more complex - if it could be done at all.

The gain is given by

$$G(\theta, \phi) = \frac{U(\theta, \phi)}{\frac{1}{4\pi} P_{in}} \quad (4-8)$$

where P_{in} is the total power input at the antenna terminals. Both the antenna impedance and the current must be known to find this. A current has been assumed but the impedance would depend heavily on the type of cable used, the parameters of the ground, and the depth of burial.

As a result of these problems, the patterns shown are "floating". That is, their absolute values cannot be compared, but the relative values of one pattern can be. Therefore, the numbers given for the magnitudes of the patterns show only the relative values of a pattern.

Losses

Because the soil is not a perfect dielectric, it will absorb a portion of the power as the wave propagates through. The attenuation constant for a slightly lossy dielectric is given in Ramo et al (Ref 17:335) as

$$\alpha \approx \frac{k_g \epsilon''}{2\epsilon'} \quad (4-9)$$

where $\epsilon' = \epsilon_r \epsilon_0$ and $\epsilon'' = \sigma_g / \omega$. The power loss will then be

$$\gamma_1 = (\exp(-\alpha d))^2 = \left(\exp\left(-\frac{k_g \sigma_g}{2\omega \epsilon_g \epsilon_0} \frac{h}{\cos\theta_g}\right) \right)^2 \quad (4-10)$$

where $h/\cos\theta_g$ is the distance the wave travels through the ground. But for $n_g \geq 3.0$, $\cos\theta_g \approx 1$. Then, using $k_g = \sqrt{\epsilon_g} k_0$, and $\eta_0 = k_0 / \omega \epsilon_0$, equation (4-10) simplifies to

$$\gamma_1 = \exp\left(-\frac{\eta_0 \sigma_g h}{\sqrt{\epsilon_g}}\right) \quad (4-11)$$

Table IV-1 shows the loss for the different soil parameters found in the literature.

Reference	Soil moisture content	Analysis frequency	Dielectric constant ϵ_r	Conductivity (mhos/m)	Losses (dB) burial - 0.5 m
Biggs and Swarm (Ref 3:206)	not given	LF	10	0.0005	-0.13
Entzminger et al (Ref 6:45-48)	wet?	10 MHz	60	0.03	-3.2
King and Shen (Ref 10:1052)	dry	144 MHz	4	0.00004	-0.01
Corvus (Ref :33)	dry	HF, VHF	9	0.001	-1.3
	wet	HF, VHF	25	0.01	-9.2
Burke et al (Ref :99)	dry	HF, VHF	9	0.005	-0.27
	wet	HF, VHF	20	0.05	-1.7

Table IV-1. Soil Losses at a Burial Depth of 0.5 Meters.

V. Conclusions and Recommendations

Conclusions

As stated in the introduction, a goal of this thesis was to develop a simple but accurate method to determine the far-field pattern of a buried HED. A relatively simple method has been developed, but its accuracy has yet to be determined, especially since a comparison with measurements would be required.

The literature search revealed a number of articles on the topic. Most includes assumptions so that they could not be applied to this case of a HED operated at 37.5 MHz.

The solution developed in Chapter III involves conventional antenna theory and ray-optics. It assumes the ground to be a slightly lossy dielectric, which was shown to be a fairly good approximation, depending on the moisture content of the soil. The difference between this solution and the most applicable solution from the literature is a factor of $\cos\theta_a$ where θ_a is the angle off the normal to the ground. So at least overhead, the two solutions are in agreement. Near the horizon, the difference is fairly large.

The directivity or gain was not evaluated because of the difficulty of finding the total radiated or input power. Several patterns were shown for the expected current distributions. Burial seems to lower the pattern overhead so most of the power is radiated close to the horizon. Most importantly, it was shown that the pattern is dependant on the dielectric constant of the soil and how it affects

the current distribution.

Recommendations

In order to more fully compare what happens when an antenna is buried, the program in Appendix B should be expanded to integrate the pattern over the whole sphere surrounding the antenna. This would give a value for the total power radiated, and hence, the directivity could be determined. Also it would be interesting to find out exactly what happens to the current distribution and impedance on an antenna as it is buried.

The difference between the Biggs and Swarm equation and the dielectric method should be examined to find why they are the same overhead but different at the horizon. Finally, it would be good to get Vaziri's program to work and compare those results. These tools could then be used to more effectively evaluate the buried antenna array of Part II.

Bibliography

1. Sommerfeld, A. "Uber de Ausbreitung der Wellen in der Drahtlosen Telegraphic," Ann. Physic, 28 (1909).
2. Biggs, A. W. "Radiation Fields from a Horizontal Electric Dipole in a Semi-Infinite Conducting Medium," IRE Trans. on Ant. and Prop., AP-10: 358-362 (July 1962).
3. Biggs, A. W. and H. M. Swarm. "Radiation Fields of an Inclined Electric Dipole Immersed in a Semi-Infinite Conducting Medium," IEEE Trans. on Ant. and Prop., AP-11: 306-310 (May 1963).
4. Biggs A. W. and H. M. Swarm. "Radiation Fields from an Electric Dipole Antenna in Homogenous Antarctic Terrain," IEEE Trans. on Ant. and Prop., AP-16: 201-208 (March 1968).
5. Biggs A. W. and H. M. Swarm. Analytical Study of the Radiation Fields from an Electric Dipole in Stratified and Inhomogeneous Terrain. Tech Rpt. No. 98. College of Engineering, University of Washington, September, 1965.
6. Entzminger, J. N., T. F. Treadway, and S. H. Talbot. Measured Performance of HF Subsurface Dipoles. RADC-TR-69-221. Technical Report. Griffiss AFB, NY: Rome Air Development Center, June 1969.
7. Banos, A., Jr. Dipole Radiation in the Presence of a Conducting Half-Space. Oxford: Pergamon Press, 1966.
8. Vaziri, F. Electromagnetic Fields of Underground Antennas. PhD Dissertation. Dept. of Electrical Engineering, University of Houston, May 1979.
9. King, R. W. P., B. H. Sandler, and L. C. Shen. A Comprehensive Study of Subsurface Propagation From Horizontal Electric Dipole. ENG-76-17596. Dept. of Electrical Engineering, University of Houston. National Science Foundation Grant, June 1979.
10. King, R. W. P. and L. C. Shen. "Radiation into the Air Above a Horizontal Electric Dipole in the Presence of a Conducting Half-Space," Radio Science, 14 (6): 1049-1056 (Nov-Dec 1979).
11. Bannister, P. R. "The Image Theory EM fields of a Horizontal Electric Dipole in the Presence of a Conducting Half-Space," Radio Science, 17 (5): 1095-1102 (Sept-Oct 1982).
12. Miller, E. K. and G. J. Burke. Radiation From Buried Antennas. UCID-15890. Livermore Cal.: Lawrence Radiation Laboratory, University of California, August, 1971.

13. Miller, E. K. and F. J. Deadrick. Analysis of Wire Antennas in the Presence of a Conducting Half-Space. UCRL-52228. Livermore, Cal.: Lawrence Radiation Laboratory, University of California, February, 1977.
14. Brammer, D. J. Buried Insulated Antennas. RSRE-MEMO-3418. Malvern, England: Royal Signals and Radar Establishment, October 1981.
15. Stutzman, W. L. and G. A. Thiele. Antenna Theory and Design. New York: John Wiley and Sons, 1981.
16. Hecht, E. and A. Zafac. Optics. Reading, Mass: Addison-Wesley Publishing Co., 1979.
17. Ramo S., J R. Whinnery, and T. Van Duzer. Fields and Waves In Communication Electronics. New York: John Wiley and Sons, 1965.
18. Vaziri, F., S. C. F. Huang, S. A. Long, and L. C. Shen. "Measurement of the Radiated Fields of a Buried Antenna At VHF," Radio Science, 15 (4): 743-747 (July-Aug 1980).
19. Richmond, J. H., N. N. Wang, and H. B. Tran. "Propagation of Surface Waves on a Buried Coaxial Cable with Periodic Slots," IEEE Trans. on EMC, 23 (3): 139+ (Aug 1981).
20. Fitzgerald, R. G. and L. L. Haidle. "Four UHF Antennas Buried Beneath Refractory Concrete, Discussing Design, Fabrication and Power Gain and Azimuthal Pattern Measurements," IEEE Trans. on Ant. and Prop., AP-20: 56-62 (January 1972).
21. Hardened Antenna Studies, , AD-607-419. Tech. Doc. Rpt. No. RADC-TDR-64-184. Griffiss AFB, NY: Communications Techniques Branch, Rome Air Development Center, October 1964.
22. Hause, L. G., F. G. Kimmett, and P. L. McQuate. UHF Propagation Measurements from Elevated to Buried Antennas, AD-699209. Boulder, Colo.: Institute for Telecommunication Sciences, December 1969.
23. Lavrov, G. A. Near Earth and Buried Antennas. JPRS Translation No. 41, 131, 27 May 67.
24. Schwering, F. Insulated Subsurface Horizontal Wire. AD-A027504. Fort Monmouth, N.J.: Army Electronics Command, Communication/Automatic Data Processing Lab, May 1976.
25. Lien, R. H. "Radiation from a Horizontal Dipole in a Semi-Infinite Dissipative Medium," Journal of Applied Physics, 24 (1): 1-4 (January 1953).
26. King, R. W. P. and C. W. Harrison. "The Transmission of Electromagnetic Pulses into the Earth," Journal of Applied Physics, 39 (9): 4444-4452 (August 1968).

27. "Theory of Wave Propagation Along a Thin Wire Parellel to an Inter-
face," Radio Science, 7 (6): 675-679 (Jan 1972).
28. Wait, J. R., and David A. Hill. "Fields of a Horizontal Loop of
Arbitrary Shape Buried in Two-Layer Earth," Radio Science, 15 (5):
903-912 (Sept-Oct 1980).
29. Cavalcante, G. P. S. and A. J. Giarola. "Optimization of Radio
Communication in Media with Three Layers," IEEE Trans. on Ant. and
Prop., AP-31 (1): 141-144 (January 1983).
30. "Extension of Quasi-Static Range Finitely Conducting Earth Image
Theory Techniques to Other Ranges," IEEE Trans. on Ant. and Prop.,
AP-26 (3): 507-508.
31. Kraichman, M. B. Handbook of Electromagnetic Propagation in
Conduction Media. Wash. D. C.: U. S. Government Printing Office, '70.
32. Siegel, M. and R. W. P. King. "Electromagnetic Fields in a
Dissipative Half-Space, A Numerical Approach," J. Appl. Phys., 41:
2415-2423 (1970).
33. Wait, J. P. "Electromagnetic Wave Propagation Along a Buried
Insulated Wire," Canadian J. Phys., 50 (20): 2402-2409 (October
1972).
34. Weeks, W. L. and R. C. Fenwick. Submerged Antenna Report. Dallas,
Texas: Collins Radio Co. Report CER-T1477, (May 1962).
35. Special Issue on Electromagnetic Waves in the Earth, IEEE Trans. on
Ant. and Prop., AP-11 (3) (May 1963).
36. Iizuka, K. "An Experimental Investigation on the Behavior of the
Dipole Antenna Near the Interface Between the Conducting Medium
and Free Space," IEEE Trans. on Ant. and Prop., AP-12 (June 1964).
37. Wait, J. R. "Electromagnetic Fields of Sources in Lossy Media," in
Antenna Theory, (R. E. Collin and F. J. Zucker, Eds.) Part II, New
York: McGraw-Hill Book Company, pp. 438-514, 1969.
38. Schwering, Resonance Length and Input Impedance of Horizontal
Dipole Antennas Buried at Shallow Depth, Memorandum for Record,
ECOM, Fort Monmouth, N. J., March 1974.
39. Wu., T. T., R. W. P. King, and D. V. Giri, "The Insulated Dipole
Antenna in a Relatively Dense Medium," Radio Science, 8: 699-709
(July 1973).
40. Rommel, T. A. Underground Antenna Systems Design Handbook.
Report No. D2-13588. Seattle Wash.: Boeing Co., June 1962.
41. Guy, A. W. Expermental Data on Buried Antennas. Report No.
D2-90051. Seattle, Wash.: Boeing Co. January 1962.

42. Wu, T. T., and R. W. P. King. "The Dipole Antenna With Excentric Coating in a Relatively Dense Medium," IEEE Trans. on Ant. and Prop., AP-23: 57-62 (January 1975).
43. King, R. W. P., and G. S. Smith. Antennas in Matter. MIT Press, 1981.

Appendix A

Vaziri's Program

```
*****
* Main program to calculate the far-field pattern      *
* using F. Vaziri's program                          *
* 1) Reads data from 'datath'                        *
* 2) Calls Vaziri's solution for each point in the *
*    desired pattern                                 *
* 3) Formats data for plotting                       *
*****
real N,X(5,0:90),Y(5,0:90)
data ((Y(i,j),j=0,90),i=1,5)/455*-50./
open (1,file='datath')
rewind 1

read(1,1) Nplots,Id
1      format(2i3)
30     write(6,2) Id, Nplots
2      format(///// '#',i2,5x,i3,' plots')

write(6,3)
3      format('/ plot',3x,'N',9x,'Sg',8x,'p  ')

*****
* do loop to plot different cases on the same graph *
*****

do 10 Ip=1, Nplots

read(1,4) N,p,Sg
4      format(3f10.5)

write(6,5) Ip,N,Sg,p
5      format(i2,5f10.3,2i10)

*****
* do loop to vary XI from 0-90 degrees *
*****
50     do 20 IXI=5,85,5
XIId=IXI+.0001

call Pviz(XIId,N,Sg,Pw,p)

Y(Ip,IXI)=Pw
X(Ip,IXI)=XIId
```

```
        if(Pw.ge.1e3)goto 10
20      continue
10      continue

        write(6,8)
8        format(//15x,'1',9x,'2',9x,'3',9x,'4',9x,'5')
        write(6,9) (X(1,1),(Y(j,1),j=1,5),1=0,90,5)
9        format(6f10.3)

        read(1,1) Nplots,Id
        if(Id.ne.0)goto 30

        stop
        end
```

```

      subroutine Pviz(XId,N,Sg,Pw,p)
      *****
      * this subroutine calculates the far-field radiation intensity *
      * using a modified program from a dissertation by F. Vaziri. *
      *****

      *****
      * Input from main program *
      * XId angle off horizon (degrees) *
      * N index of refraction for ground *
      * Sg conductivity of the ground *
      * p distance from antenna *
      * Output *
      * Pw radiation intensity *
      *****

      real N
      DIMENSION INDEX(6)
      COMMON NN,NX,XNEAR,XINTER,XFAR
      COMMON /BLK1/H,Z,FQ,ER1,SIG1,MU1,ER2,SIG2,MU2,SIGN,R,W2MUO,EIOM
      common /b4/Eint

      *****
      * INDEX indicates which polarization *
      * H burial depth *
      * FQ operating frequency *
      *****
      data PI/3.1415926536/
      DATA INDEX/0,0,1,0,0,0/
      DATA H,FQ/.175,144.E6/

      *****
      * ER1, SIG1 dielectric constant and conductivity of the *
      * half-space that includes the antenna *
      * ER2, SIG2 dielectric constant and conductivity of the *
      * half-space opposite the antenna *
      *****
      ER1=N*N
      SIG1=Sg
      DATA ER2,SIG2/1.0,0.0/

      CALL CONST

      *****
      * convert deg to rad *
      *****
      XIr=XId*PI/180.

      *****
      * Z vertical observation distance *
      * R horizontal observation distance *
      * the coordinate system is upside- *
      * down because H must be positive *

```

Z=-p*sin(XIr)
R=p*cos(XIr)

4 DO 4 NN=1,6
CALL COMP(INDEX(NN))

* calculate radition intensity *

Pw=Eint*Eint/(2*377)

6 return
END
Z

SUBROUTINE CONST

C THIS SUBROUTINE CALCULATES NECESSARY CONSTANTS.

COMMON /BLK1/H,Z,FQ,ER1,SIG1,MU1,ER2,SIG2,MU2,SIGN,R,W2MUO,EO
COMMON /BLK2/W,KO,N1SQ,N2SQ,E1,E2,K1,K2,K1S,K2S,N,CSIG,POLE,P

C MUO,EO,ABSN

COMMON /BLK4/AI,AIK1,AIK2

COMMON /BLK6/ KR,E1INV

COMPLEX N1SQ,N2SQ,E1,E2,N1,N2,K1,K2,N,CSIG ,K1S,K2S

COMPLEX KR,E1INV

REAL KO,MUO,MU1,MU2

EO=8.854E-12
MUO=1.257E-06
PI=3.14159

C MU1 AND MU2 ARE RELATIVE PERMEABILITIES OF MEDIUM 1 AND 2

MU1=1.
MU2=1.

1 IF(2) 1,2,2
SIGN=-1
GO TO 3
2 SIGN=1.
3 CONTINUE

W=2.*PI*FQ
C=1./(EO*MUO)**.5
W2MUO=W*W*MUO
EOINV=1./EO
KO=W/C

N1SQ=CMPLX(ER1,SIG1/W/EO)
E1=EO*N1SQ
N1=CSQRT(N1SQ)
K1=KO*N1
AIK1=AIMAG(K1)
K1S=K1*K1

N2SQ=CMPLX(ER2,SIG2/W/EO)
E2=EO*N2SQ
N2=CSQRT(N2SQ)
K2=KO*N2
AIK2=AIMAG(K2)
K2S=K2*K2

```
E1INV=1./E2
KR=E1/E2
N=K2/K1
ABSN=CABS(N)
CSIG=CMPLX(SIG1,-E0*W)
POLE=AIMAG(CSQRT((E2*E2*K1S-E1*E1*K2S)/(E2*E2-E1*E1)))
```

```
RETURN
END
```

z

SUBROUTINE COMP(INDEX)

C THIS SUBROUTINE EVALUATES THE FIELD COMPONENT IF INDEX NE 0

COMMON NN,NX,XNFAR,XINTER,XFAR
COMMON /BLK1/H,Z,FQ,ER1,SIG1,MU1,ER2,SIG2,MU2,SIGN,R,W2MUPO,EO
COMMON /BLK2/W,KO,N1SQ,N2SQ,E1,E2,K1,K2,K1S,K2S,N,CSIG,POLE,P

C MUO,EO,ABSN

COMMON /BLK3/CONST.
COMMON /BLK4/AI,AIK1,AIK2
COMMON /BLK5/IFLG1,IFLG2
common /b4/Eint

COMPLEX N1SQ,N2SQ,E1,E2,K1,K2,N,CSIG,K1S,K2S
COMPLEX I1,I2,I,CONST

REAL KO,MUO

IF (INDEX.EQ.0) GO TO 5
IFLG1=0
IFLG2=0
EPS=0.
I1=(0.,0.)
I2=(0.,0.)
START=0.
END=.99*POLE

C INTEGRATE FROM 0 TO THE VICINITY OF THE POLE

CALL AUTO(START,END,EPS,I1,I2)
START=END
END=1.005*POLE

C INTEGRATE ON THE POLE

CALL AUTO(START,END,EPS,I1,I2)
START=END
END=1.015*POLE
IFLG1=0
IFLG2=0
CALL AUTO(START,END,EPS,I1,I2)
IFLG1=0
IFLG2=0
START=END

C CONTINUE INTEGRATION

DO 2 J=1,41,4
AJ=J

END=POLE*(2.**AJ)

C TERMINATE INTEGRATION IF INTEGRAND IS NEGLIGIBLE

IF (IFLG1+IFLG2-2) 1,3,3

1 CALL AUTO(START,END,EPS,I1,I2)

2 START=END

3 CONTINUE

I=I1+I2

Eint=cabs(I*CONST)

5 RETURN

END

%

SUBROUTINE AUTO(START,END,EPX,I1,I2)

C THIS SUBROUTINE PERFORMS NUMERICAL INTEGRATION ALONG VERTIC
C BRANCH CUTS.

COMMON NN,NX
COMMON /BLK1/H,Z,FQ,ER1,SIG1,MU1,ER2,SIG2,MU2,SIGN,R,W2MUO,EO
COMMON /BLK4/AI,AIK1,AIK2
COMMON/BLK5/IFLG1,IFLG2

COMPLEX I1,I2,T1,T2,CSIQD,FNC

EXTERNAL FNC

C ETA IS INTEGRATION ERROR

ETA=.01
NX=1
AJ=AJK1
IF((Z+H).LT.0.) NX=3

C TERMINATE INTEGRATION ALONG BRANCH CUT 1 IF INTEGRAND TOO S

IF (IFLG1.EQ.1) GO TO 1
T1=CSIQD(START,END,FNC,EPX,ETA)
I1=I1+T1
IF (CABS(T1).LT.CABS(I1)*.01) IFLG1=1
1 CONTINUE

NX=NX+1
AI=AIK2

C TERMINATE INTEGRATION ALONG BRANCH CUT 2 IF INTEGRAND TOO S

IF (IFLG2.EQ.1) GO TO 2
T2=CSIQD(START,END,FNC,EPX,ETA)
I2=I2+T2
IF (CABS(T2).LT.CABS(I2)*.01) IFLG2=1
2 CONTINUE
EPX=CABS(I1+I2)*.001
RETURN
END

X

COMPLEX FUNCTION FNC(X)

C THIS FUNCTION SUBPROGRAM EVALUATES THE NUMERICAL VALUE OF THE
 C INTEGRAND. WHEN ARGUMENT IS ZERO, IT ALSO CALCULATES
 C CORRESPONDING BANOS'S APPROXIMATIONS.

dimension JFLG(6)

COMMON NN,NX,XNEAR,XINTER,XFAR
 COMMON /BLK1/H,Z,FQ,ER1,SIG1,MU1,ER2,SIG2,MU2,SIGN,R,W2MUO,EOI
 COMMON /BLK2/W,KO,N1SQ,N2SQ,E1,E2,K1,K2,K1S,K2S,N,CSIG,POLE,PI
 C MUO,EO,ABSN
 COMMON/BLK3/CONST
 COMMON /BLK4/AI,ATK1,ATK2
 COMMON /BLK6/ KR,E1INV

COMPLEX KR,KRA2,KRB2,E1INV
 COMPLEX N1SQ,N2SQ,E1,E2,K1,K2,N,CSIG,K1S,K2S
 COMPLEX B1,B2,L,ARG,EXP1,EXP2,FRAC1,FRAC2,A1,A2
 COMPLEX XFRAC1,XFRAC2,CONST
 complex T
 COMPLEX HONE0,HONE1
 COMPLEX HO,H1,H1D,FX1,FX2

REAL KO,MUO,MU1,MU2

DATA JFLG/1,1,0,1,1,-1/

IF(X.GT.1.E-30) GO TO 1
 FNC=(0.,0.)

C CALCULATE OBSERVER HEIGHT FOR BANOS'S APPROXIMATIONS.

Z1=Z-H

C SKIP BANOS'S APPROXIMATIONS IF SOURCE DIPOLE IS IN AIR

IF (ABSN.GT.1.) GO TO 180
 T=(0.,1.)*N*CSQRT(.5*PI*(0.,1.)*K2*R)
 180 IF((Z+H).LT.0.) GO TO 72
 1 IF (R*(AI+X).LE.20.) GO TO (3,4,6,7),NX
 FNC=(0.,0.)
 RETURN

C EVALUATE FIELD INTEGRAL ALONG BRANCH CUT 1 FOR POINTS OF
 C OBSERVATION IN MEDIUM

3 - R1=CSQRT(X*X-(0.,2.)*K1*X)

```
print*, "at 3"  
B2=CSQRT(K2S-K1S+X*X-(0.,2.)*K1*X)  
L=K1+(0.,1.)*X
```

C USE MODIFIED FORMULAS IF SOURCE DIPOLE IN AIR

```
IF (ABSN.GT.1.) B2=-B2  
EXP1=CEXP((0.,-1.)*B1*SIGN*7)  
EXP2=CEXP((0.,1.)*B1*(Z+2.*H))  
KRB2=KR*B2  
ARG=L*R  
IF (JFLG(NN)) 200,210,220  
220 H0=HONE0(ARG)  
H1=HONE1(ARG)  
H1D=H0-H1/ARG  
FRAC1=(B1+B2)/(B1-B2)  
FX1=FRAC1*EXP2  
210 FRAC2=(B1+KRB2)/(B1-KRB2)  
FX2=FRAC2*EXP2  
GO TO 230  
200 FRAC1=(B1+B2)/(B1-B2)  
FX1=FRAC1*EXP2  
230 continue
```

C EVALUATE FIELD INTEGRAL ALONG BRANCH CUT 2 FOR POINTS OF
OBSERVATION IN MEDIUM 1

```
4 A1=CSQRT(K1S-K2S+X*X-(0.,2.)*K2*X)  
print*, "at 4"  
A2=CSQRT(X*X-(0.,2.)*K2*X)  
L=K2+(0.,1.)*X
```

C USE MODIFIED FORMULAS IF SOURCE DIPOLE IN AIR

```
IF (ABSN.GT.1.) A1=-A1  
EXP2=CEXP((0.,1.)*A1*(Z+2.*H))  
KRA2=KR*A2  
ARG=L*R  
IF (JFLG(NN)) 300,310,320  
320 H0=HONE0(ARG)  
H1=HONE1(ARG)  
H1D=H0-H1/ARG  
FRAC1=(A1+A2)/(A1-A2)  
310 FRAC2=(A1+KRA2)/(A1-KRA2)  
GO TO 330  
300 FRAC1=(A1+A2)/(A1-A2)  
330 continue
```

C EVALUATE FIELD INTEGRAL ALONG BRANCH CUT 1 FOR POINTS OF
OBSERVATION IN MEDIUM 2

```
6 B1=CSQRT(X*X-(0.,2.)*K1*X)  
B2=CSQRT(K2S-K1S+X*X-(0.,2.)*K1*X)
```

L=K1+(0.,.61.)*X
L=K1+(0.,.1.)*X

C USE MODIFIED FORMULAS IF SOURCE DIPOLE IN AIR

IF (ABS.N.GT.1.) B2=-B2
EXP1=CEXP((0.,.1.)*B1*H)
EXP2=CEXP((0.,.1.)*B2*(Z+H))
KRB2=KR*B2
ARG=L*R
IF (JFLG(NN)) 400,410,420
420 H0=HONE0(ARG)
H1=HONE1(ARG)
H1D=H0-H1/ARG
FRAC1=1./(B1+B2)
FRAC2=1./(B1-B2)
410 XFRAC1=E1INV/(B1+KRB2)
XFRAC2=E1INV/(B1-KRB2)
GO TO 430
400 FRAC1=1./(B1+B2)
FRAC2=1./(B1-B2)
430 GO TO 70

C EVALUATE FIELD INTEGRAL ALONG BRANCH CUT 2 FOR POINTS OF
C OBSERVATION IN MEDIUM 2

7 A1=CSQRT(K1S-K2S+X*X-(0.,.2.)*K2*X)
A2=CSQRT(X*X-(0.,.2.)*K2*X)
L=K2+(0.,.1.)*X

C USE MODIFIED FORMULAS IF SOURCE DIPOLE IN AIR

IF (ABS.N.GT.1.) A1=-A1
EXP1=CEXP((0.,.1.)*A1*H)
EXP2=CEXP((0.,.1.)*A2*(Z+H))
KRA2=KR*A2
ARG=L*R
IF (JFLG(NN)) 500,510,520
520 H0=HONE0(ARG)
H1=HONE1(ARG)
H1D=H0-H1/ARG
FRAC1=1./(A1+A2)
FRAC2=1./(A1-A2)
510 XFRAC1=E1INV/(A1+KRA2)
XFRAC2=E1INV/(A1-KRA2)
GO TO 530
500 FRAC1=1./(A1+A2)
FRAC2=1./(A1-A2)
530 GO TO 71

C *****
C HED Ez2
C *****

```
70 FNC=L*L*HONE1(ARG)*EXP2*B1*(XFRAC1/EXP1-XFRAC2*EXP1)
RETURN
71 FNC=L*L*HONE1(ARG)*A1*EXP1*(XFRAC2*EXP2-XFRAC1/EXP2)
RETURN
72 CONST=1./(4.*PI*W)
IF(ABSN.GT.1.) RETURN

XNEAR =CABS(K1/(2.*PI*CSIG*R*R))
XINTER=CABS(K2*K2/(2.*PI*CSIG*R)/N*(1.+T))
XFAR =CABS(K1/(2.*PI*CSIG*N*N*R*R))

RETURN
END
```

Z

COMPLEX FUNCTION CSIQD(A,B,FCN,EPS,ETA)

```

C      ROMBERG INTEGRATION FOR COMPLEX FUNCTION WITH REAL
C      ARGUMENT, MODIFIED

COMPLEX FCN,Q(11),T,SUM,FCNXI,QX1,QX2
EXTERNAL FCN
H=(B-A)/2.
T=H*(FCN(A)+FCN(B))
NX=2
DO 12 N=1,10
SUM=0.
DO 2 I=1,NX,2
FCNXI=FCN(A+FLOAT(I)*H)
2  SUM=SUM+FCNXI
T=T/2.+H*SUM
Q(N)=(T+H*SUM)/1.5
IF(N-2) 10,3,3
3  F=4.
I=N
DO 4 J=2,N
I=I-1
F=F*4.
4  Q(I)=Q(I+1)+(Q(I+1)-Q(I))/(F-1.)
IF(N-3)9,6,6
6  X1=ABS(REAL(Q(I)-QX2))+ABS(REAL(QX2-QX1))
X2=ABS(AIMAG(Q(I)-QX2))+ABS(AIMAG(QX2-QX1))
TABS1=ABS(REAL(Q(I)))
TABS2=ABS(AIMAG(Q(I)))
IF(TABS1)7,8,7
7  IF(X1/TABS1-ETA)20,20,8
8  IF(X1-EPS)20,20,9
20 IF(TABS2)71,81,71
71 IF(X2/TABS2-ETA)11,11,81
81 IF(X2-EPS)11,11,9
9  QX1=QX2
10 QX2=Q(1)
H=H/2.
12 NX=NX*2.
WRITE(6,100) A,B
100 FORMAT(43H ACCURACY LESS THAN SPECIFIED VALUES--CSIQD 2E11.4)
11  CSIQD=Q(1)
RETURN
END

```

Z

COMPLEX FUNCTION HONE0(XZ)

C

HANKEL FUNCTION OF FIRST KIND, ORDER 0, IMAGINARY PART LT 30

IMPLICIT COMPLEX (X)

AIXZ=AIMAG(XZ)

IF(AIXZ.GT.20.) GO TO 81

XW=-XZ*XZ/4.

PI=3.141592653589

TPI=2.*PI

XI=(0.,1.)

IF(CABS(XZ).GT.5.) GO TO 7

FAC=0.

XFAC=(1.,0.)

XSUMY=(0.,0.)

XSUMJ=(1.,0.)

DO 5 I=1,50

AI=I

FAC=FAC+1./AI

XFAC=XFAC*XW/(AI*AI)

XTE=FAC*XFAC

XSUM7=XSUMY+XTE

XSUMJ=XSUMJ+XFAC

IF(CABS(XTE).LT.1.E-10) GO TO 6

5

CONTINUE

WRITE(6,92)XZ,XTE,XFAC

92

FORMAT(5X,'HONE0 SUM EXCEEDS 50 TERMS',6E15.3//)

HONE0=(0.,0.)

RETURN

6

XJ=XSUMJ

HONE0=XJ+XI*(2./PI)*((CLOG(XZ/2.)+.5772156649)*XJ-XSUMY)

RETURN

7

XP=1.-(9./(128.*XZ*XZ))*(1.-1225./(768.*XZ*XZ))

XQ=- (1./(8.*XZ))*(1.-225./(384.*XZ*XZ))

RZ=REAL(XZ)

SIGN=1.

IF(RZ.LT.0.)SIGN=-1.

71

IF(ABS(RZ).LT.TPI) GO TO 73

72

RZ=RZ-SIGN*TPI

GO TO 71

73

HONE0=(XP+XI*XQ)*(COS(RZ-.25*PI)+XI*SIN(RZ+.25*PI))

1 *EXP(-AIXZ)*CSQRT(2./(PI*XZ))

RETURN

81

HONE0=(0.,0.)

RETURN

END

Z

COMPLEX FUNCTION HONE1(XZ)

C HANKEL FUNCTION OF FIRST KIND, ORDER 1, IMAGINARY PART LT 30

```

IMPLICIT COMPLEX(X)
AIXZ=AIMAG(XZ)
IF(AIXZ.GT.20.) GO TO 81
XW=-XZ*XZ/4.
PI=3.141592653589
TPI=2.*PI
XI=(0.,1.)
IF(CABS(XZ).GT.5.) GO TO 7
FAC=-.5772156649
XFAC=(1.,0.)
XSUMY=FAC+.5
XSUMJ=(1.,0.)
DO 5 I=1,50
AI=I
FAC=FAC+1./AI
XFAC=XFAC*XW/(AI*(AI+1.))
XTE=(FAC+.5/(AI+1.))*XFAC
XSUMY=XSUMY+XTE
XSUMJ=XSUMJ+XFAC
IF(CABS(XTE).LT.1.E-10) GO TO 6
5 CONTINUE

WRITE(6,92)XZ,XTE,XFAC

92 FORMAT(5X,'XHFR1 SUM EXCEEDS 50 TERMS',6E15.3//)
HONE1=(0.,0.)
RETURN
6 XJ=XSUMJ*XZ/2.
HONE1=XI*((CLOG(XZ/2.)*XJ-1./XZ)*(2./PI)-XZ*XSUMY/PI)+XJ
RETURN
7 XP=1.+(15./(128.*XZ*XZ))*(1.-315./(256.*XZ*XZ))
XQ=(3./(8.*XZ))*(1.-35./(128.*XZ*XZ))
RZ=REAL(X7)
SIGN=1.
IF(RZ.LT.0.)SIGN=-1.
71 IF (ABS(RZ).LT.TPI) GO TO 73
72 R7=RZ-SIGN*TPI
GO TO 71
73 HONE1=(XP+XI*XQ)*(COS(RZ-.75*PI)+XI*SIN(RZ-.75*PI))*
C EXP(-AIXZ)*CSQRT(2./(PI*XZ))
RETURN
81 HONE1=(0.,0.)
RETURN
END
Z

```

Appendix B

Dielectric Method Program
program vertic

```
*****
* Main program used to calculate the far-field pattern          *
* of a horizontal electric dipole.                             *
* 1) Reads data for current distribution and soil parameters  *
* 2) Calls Uff subroutine to calculate the radiation          *
*    intensity at each point in the pattern.                 *
* 3) Formats data for plotting                                *
*    (plotting subroutine not shown)                          *
*****
```

```
real N,Kr,X(5,0:180),UdB(5,0:180),U(2)
common /b1/ALP,Kr,shift
data PI/3.1415926536/

open (1,file='datath')
rewind 1

read(1,1) Nplots,Id
1 format(2i3)

open(2,file='outhth')
30 write(2,2) Id, Nplots :
2 format(/////'#',i2,5x,i3,' plots')

write(2,3)
3 format('/ plot',6x,'Meth',6x,'J',9x,'N',9x,'B',9x,'ALP',7x
c,'Kr',8x,'PHId',8x,'shift'/)
```

```
*****
* initialize                                                    *
* UdB power density pattern (in dB's),                        *
* Gerr greatest integration error per graph                   *
*****
do 50 i=0,180
do 50 j=1,5
UdB(j,i)=0.
50 continue
Gerr=1e-5
```

```
*****
* do loop to plot different cases on the same graph          *
*****
do 10 Ip=1, Nplots

read(1,4) Meth,J,N,B,ALP,Kr,PHId,shift
4 format(2i3,6f10.5)

write(2,5) Ip,Meth,J,N,B,ALP,Kr,PHId,shift
```

```

5      format(i5,2i10,6f10.3)

*****
* do loop to vary XId (the angle off the horizon) *
* from 0-90 degrees for the front lobe and then *
* 90-0 degrees for the back lobe *
*****
      do 20 IXId=0,180
        XId=IXId+.0001
        if (IXId.gt.90) then
          PHId=180.
          XId=180-IXId+.0001
        end if

        call Uff(PHId,XId,N,J,B,Err,U(1),U(2))

        UdB(Ip,IXId)=10.*alog10(U(Meth)+1e-5)
        X(Ip,IXId)=IXId

        if(Err.gt.Gerr) Gerr=Err
20      continue
10      continue

      write(2,11) GERR
11      format(' greatest integration error=',f10.5///)

*****
* MPLOTS plotting subroutine *
* HDCOPY transfers plot to paper using Textronix 4631 *
* Hard Copy Unit *
*****

      call MPLOTS(5,181,X,UdB,UdBmax)

      write(6,6) Id
6      format(i3)
      call HDCOPY

*****
* test for next set of data *
*****

      read(1,1) Nplots,Id
      if(Id.ne.0)goto 30

40     stop
      end

Z

```

subroutine Uff(PHId,XId,Ng,J,B,Err,Upd,Ubs)

```
*****
* Input
*   B   length of antenna (meters)
*   PHId azimuthal angle (degrees)
*   J   polarization index
*       J=1 for theta polarization
*       J=2 for horizontal
*   XId angle off horizon (degrees)
*   Ng  index of refraction for ground
* Output
*   Upd radiation intensity (perfect dielectric method)
*   Ubs radiation intensity (Biggs and Swarm method)
*   Err max integration error per case
* Output to INT
*   THa,PHIr
*****
```

```
external INT
common /b2/THa,PHIr
real Ng,Na,E(2),Ko
complex CDM
```

```
*****
* Na  index of refraction in air
* FQ  operating frequency
* Eo  permittivity of free space
* C   speed of light (m/s)
* W   radial frequency
* Ko  propagation coefficient of free space
* ETAo intrinsic impedance of free space
*****
data Na,PI,FQ,Eo,C/1.0,3.1415926536,37.5e6,8.854e-12,3e8/
W=2*PI*FQ
Ko=W/C
ETAo=377.
```

```
*****
* convert deg to rad
*****
PHIr=PHId*PI/180.
XIr=XId*PI/180.
```

```
*****
* snell's law
* THa angle from norm in air
* THg angle from norm in ground
*****
THa=PI/2-XIr
```

THg=asin(Na*sin(THa)/Ng)

```
*****  
* transmission coefficients *  
* TT theta polarization *  
* TH horizontal polarization *  
*****
```

TT=2.*Ng*cos(THg)/(Ng*cos(THa)+Na*cos(THg))
TH=2.*Ng*cos(THg)/(Ng*cos(THg)+Na*cos(THa))

```
*****  
* integrate to find dipole moment *  
* DM - dipole moment *  
*****
```

A=0.
call INTEG(CDM,A,B,INT,Err)
DM=cabs(CDM)

```
*****  
* Perfect dielectric method *  
* E fields ( *r ) *  
* E(1) theta pol. *  
* E(2) horizontal pol. *  
*****
```

E(1)=30.*Ko*TT*DM*cos(THg)*cos(PHir)
E(2)=30.*Ko*TH*DM*sin(PHir)

Upd=1/(2.*ETAo)*E(J)*E(J)*COS(THa)/COS(THg)*((Na/Ng)**2)
Ubs=Upd*cos(THa)/cos(THg)

return
end

Z

SUBROUTINE INTEG(INTGRL,A,B,ARG,Errg)
 C INTEGRATION SUBROUTINE

```

*****
* Input                                     *
* A,B   endpoints                          *
* ARG   integrand function                 *
* Errg  greatest integration error         *
* Output                                    *
* INTGRL value of integral                 *
* Errg                                     *
*****
      EXTERNAL ARG
      COMPLEX CUM,DEL,Y(5),ARG,INTGRL,YIV
      DOUBLE PRECISION RDP,XN,RANG

      RANG=B-A
      NINIT=40
      NSTEPS=NINIT
      ERROR=0.0
      ERRMUL=1.0/180.0
3     DO 3 I=1,5
      Y(I)=0.0
      CUM=0.0
      XN=2*NSTEPS
      RDP=A
      R=RDP
      Y(1)=ARG(R)
15    DO 20 I=2,5
      RDP=RDP+RANG/XN
      R=RDP
      Y(I)=ARG(R)
20    CONTINUE
25    YIV=Y(1)+Y(5)-4.0*(Y(2)+Y(4))+6.0*Y(3)
      ERROR=ERRMUL*CABS(YIV)
26    IF(ERROR.GT.Errg) Errg=ERROR
      DEL=(Y(1)+Y(5)+4.0*(Y(2)+Y(4))+2.0*Y(3))
      DEL=RANG*DEL/(3.*XN)
      CUM=CUM+DEL
      IF((R+1.0E-5).GT.B) GO TO 80
      Y(1)=Y(5)
      DO 30 I=2,5
      RDP=RDP+RANG/XN
      R=RDP
      Y(I)=ARG(R)
30    CONTINUE
      GO TO 25
80    INTGRL=CUM
      RETURN
      end
Z

```

COMPLEX FUNCTION INT(S)
 * INTEGRAND FUNCTION

```

*****
* Input from INTEG *
* S distance on antenna *
* Input from MAIN *
* Kr relative propagation constant of antenna *
* ALP attenuation constant of antenna *
* shift phase shift for second half of array *
* Input from method subroutine(s) *
* THa angle from the normal in air (radians) *
* PHIr azimuthal angle (radians) *
*****
COMMON /b1/ALP,Kr,shift
COMMON /b2/THa,PHIr
REAL Kr,LAMo
COMPLEX ZJ,I
  
```

```

*****
* FQ operating frequency *
* C speed of light *
*****
data FQ,C,ZJ,PI/37.5e6,3e8,(0.,1.),3.1415926536/
  
```

```

*****
* LAMo - free space wavelength *
* BET - antenna propagation constant *
* BETo - free space propagation constant *
*****
LAMo=C/FQ
BET=Kr*2.*PI/LAMo
BETo=2.*PI/LAMo
  
```

```

*****
* special instructions for the array *
*****
if(S.gt.16.) then
  if(S.lt.20.) goto 10
  d=36-S
  gam=shift*PI/180.
else
  d=S
  gam=0.
end if
  
```

```

*****
* I - CURRENT ON ANTENNA *
*****
I=SIN(BET*d)*CEXP(-ALP*(16.-d)+ZJ*gam)
  
```

```
*****  
* INT - DIPOLE MOMENT *  
*****  
      INT=I*CEXP(ZJ*BETO*S*SIN(THa))*COS(PHIr))  
  
      RETURN  
  
10    INT=0  
      return  
      end  
  
Z
```

Vita

Jeffrey W. Burks was born on 28 August 1960 in Upper Sandusky, Ohio. He graduated from high school in North Robinson, Ohio in 1978 and attended the Mansfield Branch of Ohio State University in Mansfield, Ohio and Ohio University in Athens, Ohio. He received the degree of Bachelor of Electrical Engineering from Ohio University on 12 June 1982. Upon graduation, he received a commission in the USAF through the ROTC program. He entered active duty a week later as a student in the Graduate Electro-Optics program at the School of Engineering, Air Force Institute of Technology.

Permanent address

52 Crestview Dr.

Crestline, Ohio 44827

UNCLASSIFIED

SECURITY CLASSIFICATION OF THIS PAGE

REPORT DOCUMENTATION PAGE

1a. REPORT SECURITY CLASSIFICATION UNCLASSIFIED		1b. RESTRICTIVE MARKINGS	
2a. SECURITY CLASSIFICATION AUTHORITY		3. DISTRIBUTION/AVAILABILITY OF REPORT Approved for public release; distribution unlimited.	
2b. DECLASSIFICATION/DOWNGRADING SCHEDULE			
4. PERFORMING ORGANIZATION REPORT NUMBER(S) AFIT/GEO/EE/83D-1 Part I		5. MONITORING ORGANIZATION REPORT NUMBER(S)	
6a. NAME OF PERFORMING ORGANIZATION School of Engineering	6b. OFFICE SYMBOL (If applicable) AFIT/EN	7a. NAME OF MONITORING ORGANIZATION	
6c. ADDRESS (City, State and ZIP Code) Air Force Institute of Technology Wright-Patterson AFB, Ohio 45433		7b. ADDRESS (City, State and ZIP Code)	
8a. NAME OF FUNDING/SPONSORING ORGANIZATION	8b. OFFICE SYMBOL (If applicable)	9. PROCUREMENT INSTRUMENT IDENTIFICATION NUMBER	
8c. ADDRESS (City, State and ZIP Code)		10. SOURCE OF FUNDING NOS.	
11. TITLE (Include Security Classification) See Box 19		PROGRAM ELEMENT NO.	TASK NO.
12. PERSONAL AUTHOR(S) Jeffrey W. Burks, B.S., 2dLt, USAF		PROJECT NO.	WORK UNIT NO.
13a. TYPE OF REPORT MS Thesis	13b. TIME COVERED FROM _____ TO _____	14. DATE OF REPORT (Yr., Mo., Day) 1984 January	15. PAGE COUNT Part I - 67 pp.
16. SUPPLEMENTARY NOTATION Approved for public release; distribution unlimited. Lynn E. Wolan 2 Feb 84 Dean for Research and Professional Development Air Force Institute of Technology (AIC) Wright-Patterson AFB, Ohio 45433			
17. COSATI CODES		18. SUBJECT TERMS (Continue on reverse if necessary, and identify by block number)	
FIELD	GROUP	Underground Antennas, Antenna Arrays, Dipole Antennas, Antenna Radiation Patterns, Very High Frequency	
20	14		
09	05		
19. ABSTRACT (Continue on reverse if necessary and identify by block number) Title: BURIED ANTENNA ANALYSIS AT VHF PART I: THE BURIED HORIZONTAL ELECTRIC DIPOLE			
20. DISTRIBUTION/AVAILABILITY OF ABSTRACT UNCLASSIFIED/UNLIMITED <input checked="" type="checkbox"/> SAME AS RPT. <input type="checkbox"/> DTIC USERS <input type="checkbox"/>		21. ABSTRACT SECURITY CLASSIFICATION UNCLASSIFIED	
22a. NAME OF RESPONSIBLE INDIVIDUAL Thomas W. Johnson, Captain, USAF	22b. TELEPHONE NUMBER (Include Area Code) (513) 255-3576	22c. OFFICE SYMBOL AFIT/ENG	

Part I: A method was developed to find the far-field radiation pattern of a buried horizontal electric dipole (HED) at 37.5 MHz. The imaginary part of the index of refraction was shown to be negligible for dry soil at this frequency so standard antenna theory and ray-optic theory were used. The effect of the ground-air interface was modeled using the transmission coefficient and Snell's law for a dielectric interface. Because the current distribution for the buried HED depends on antenna construction, results are shown for the far-field pattern in the air for different current distributions on the HED.

The literature on this problem was reviewed; most used the Sommerfeld or moment methods to make the same calculations. The results of one of the reports using the Sommerfeld method could be compared and were found to be similar. An extensive bibliography is included.

Part II: The analysis was then applied to a buried antenna array. The current distribution was known and was used to calculate the far-field pattern. It was concluded that the far-field pattern is highly dependant on the current distribution. This part is classified.

